Methods and Resources

RUNNING HEAD: *In vivo* spatiotemporal imaging of fatty acid β-oxidation

Spatiotemporally quantitative *in vivo* imaging of mitochondrial fatty acid β-oxidation at cellular-level resolution in mice

Ayumi Matsumoto[1, 4], Isao Matsui*[, 1, 2, 4], Shohei Uchinomiya[3], Yusuke Katsuma[1], Seiichi Yasuda[1], Hiroki Okushima[1], Atsuhiro Imai[1], Takeshi Yamamoto[1], Akio Ojida[3], Kazunori Inoue[1], and Yoshitaka Isaka[1].

[1] Department of Nephrology, Osaka University Graduate School of Medicine, 2-2 Yamada-oka, Suita, Osaka 565-0871, Japan

[2] Transdimensional Life Imaging Division, Institute for Open and Transdisciplinary Research Initiatives, Osaka University, 2-1 Yamada-oka, Suita, Osaka 565-0871, Japan

[3] Department of Medical Chemistry and Chemical Biology, Graduate School of Pharmaceutical Science, Kyushu University, 3-1-1 Maidashi, Higashi-Ku, Fukuoka 812-8582, Japan

[4] These authors contributed equally

Correspondence: Isao Matsui (matsui@kid.med.osaka-u.ac.jp)

Department of Nephrology, Osaka University Graduate School of Medicine

2-2 Yamada-oka, Suita, Osaka 565-0871, Japan

Phone: +81-6-6879-3857; Fax: +81-6-6879-3230

ABSTRACT

Mitochondrial fatty acid β-oxidation (FAO) plays a key role in energy homeostasis. Several FAO evaluation methods are currently available, but they are not necessarily suitable for capturing the dynamics of FAO *in vivo* at a cellular-level spatial resolution and seconds-level time resolution. FAOBlue is a coumarin-based probe that undergoes β-oxidation to produce a fluorescent substrate, 7-hydroxycoumarin-3-(N-(2-hydroxyethyl))-carboxamide (7-HC). After confirming that 7-HC could be specifically detected using multiphoton microscopy at excitation/emission wavelength = 820/415-485 nm, wild-type C57BL/6 mice were randomly divided into control, pemafibrate, fasting (24 or 72 hours), and etomoxir groups. These mice received a single intravenous injection of FAOBlue. FAO activities in the liver of these mice were visualized using multiphoton microscopy at 4.2 seconds/frame. These approaches could visualize the difference in FAO activities between periportal and pericentral hepatocytes in the control, pemafibrate, and fasting groups. FAO velocity, which was expressed by the maximum slope of the fluorescence intensity curve, was accelerated in the pemafibrate and 72 hours fasting groups both in the periportal and the pericentral hepatocytes in comparison to the control group. Our approach revealed differences in the FAO activation mode by the two stimuli, *i.e.* pemafibrate and fasting, with pemafibrate accelerating the time of first detection of FAO-derived fluorescence. No increase in the fluorescence was observed in etomoxir-pretreated mice, confirming that FAOBlue specifically detected FAO *in vivo*. Thus, FAOBlue is useful for visualizing *in vivo* liver FAO dynamics at the single-cell level spatial resolution and seconds-level time resolution.

NEW & NOTEWORTHY

Fatty acid β-oxidation (FAO) plays a key role in energy homeostasis. Here, the authors established a strategy for visualizing FAO activity *in vivo* at the cellular-level spatial resolution and seconds-level time resolution in mice. Quantitative analysis revealed spatiotemporal heterogeneity in hepatic FAO dynamics. Our method is widely applicable because it is simple and uses a multiphoton microscope to observe the FAOBlue-injected mice.

Keywords: Fatty acid β-oxidation; *in vivo* imaging; spatiotemporal resolution; liver

INTRODUCTION

Mitochondrial fatty acid β-oxidation (FAO) is the primary metabolic pathway for the degradation of fatty acids and the maintenance of energy homeostasis.(1) Currently, there are several methods researchers use to analyze different aspects of FAO in various physiological and pathological conditions.(2–4) These include real-time PCR and immunoblots to analyze expression levels of critical FAO-related enzymes and regulators, real-time cell metabolic analysis to measure oxygen consumption rates, and mass spectrometry to analyze metabolic intermediate levels, and quantification of $^{3}H_2O$ or $^{14}CO_2$ converted from ^{3}H- or ^{14}C-labeled fatty acids.(5–10)

Subheading level 2

Understanding FAO dynamics *in vivo* is essential because inter-organ communication is critical in regulating FAO.(11, 12) However, the methods currently available are not necessarily suitable for capturing the spatiotemporal dynamics of FAO *in vivo* at the cellular-level spatial resolution and seconds-level time resolution.(13) Therefore, improvements in the FAO analysis method at these points can further enhance our understanding of FAO in pathophysiology.

Subheading level 3

Recently, we developed FAOBlue, a coumarin-based probe that can detect FAO activity in cultured cells.(14) FAOBlue is the compound described as probe **10** in our previous report, and it undergoes mitochondrial β-oxidation to produce 7-hydroxycoumarin-3-(N-(2-hydroxyethyl))-carboxamide (7-HC), a fluorescent substance described as coumarin **16** in our previous report.(14) Although we have reported that FAOBlue helps measure FAO activity *in vitro*, it was unknown whether the reagent was also helpful in measuring FAO in live animals. In this study, we established a method to evaluate the spatiotemporal dynamics of FAO *in vivo* at the cellular-level spatial resolution and seconds-level time resolution. Our method enables the visualization of FAO activity with simplicity and unprecedented spatiotemporal resolution.

MATERIALS AND METHODS

Mice studies

All animal experiments were approved by the Animal Committee of Osaka University,

Japan (approval number:02-006-006), and the study was performed in accordance with the standard guidelines regarding the use of animals in scientific experiments. Six-week-old male C57BL/6J mice were purchased from Japan SLC (RRID: IMSR_JAX:000664, Hamamatsu, Japan) and were housed in groups of 2–3 at 22–24°C in a humidity-controlled specific-pathogen-free room with a 12-hour light-dark cycle. Except for the fasting specimens, all mice had *ad libitum* access to a regular chow diet (MFG diet; Oriental Yeast, Tokyo, Japan).

Compounds preparation

FAOBlue (FDV-0033, Funakoshi, Tokyo, Japan) was dissolved in sterile-filtered dimethyl sulfoxide (DMSO, 13408-64, Nacalai Tesque Inc., Kyoto, Japan) to prepare a 10 mM stock solution aliquoted in light-proof tubes and stored at −20°C until use. At the time of use, FAOBlue was further diluted in a dilution buffer (normal saline containing 0.01% Tween-20 and 0.2% ethanol). Pemafibrate (TQ0107, TargetMol, Boston, MA, USA) was dissolved in DMSO at a concentration of 10 mg/ml to prepare a stock solution. Etomoxir (E1905, Sigma-Aldrich, St Louis, MO, USA) was dissolved in normal saline at the time of use. 7-HC was synthesized as previously described by Uchinomiya *et al*. and dissolved in DMSO to prepare a 10 mM stock solution.(14)

Experimental treatment and imaging preparations

To analyze hepatic lobule structure, Texas Red™ conjugated 70 kDa dextran (D1830, Invitrogen, Waltham, MA, USA) dissolved in normal saline at 500 μg/ml was intravenously injected (100 μl/animal) through the right jugular vein. The FAO activity was visualized with a single intravenous injection of diluted FAOBlue (62.5 μM, 100 μl/animal) through the right jugular vein. To evaluate FAO activity, the mice were randomly divided into five

groups: control (Ctrl), pemafibrate (Pema), fasting for 24 hours (Fasting_24h), fasting for 72 hours (Fasting_72h), and etomoxir (Eto). The FAO activity in the Ctrl group was evaluated without any specific pretreatment. Mice in the Pema group were administered pemafibrate (0.1 mg/kg body weight (BW)) suspended in methylcellulose 400 (133–17815, FUJIFILM Wako Pure Chemicals, Osaka, Japan) by oral gavage at 24 and 1 h before imaging. Mice in the Fasting_24h and Fasting_72h groups were fasted for 24 h and 72 h prior to imaging, respectively. Mice in the Eto group were intraperitoneally administered etomoxir (20 mg/kg BW) dissolved in normal saline at 12 h and 1 h before the imaging. All the animal experiments were performed in the morning. For *in vivo* imaging, the mice were anesthetized with an intraperitoneal injection of medetomidine, midazolam, and butorphanol. A 30-gauge catheter was inserted into the right jugular vein for reagent injection. The left lobe of the liver was exteriorized through a small flank incision and was placed on a cover glass. The microscope stage had a heater to keep the body temperature at 36–38°C. Another heater maintained the temperature inside the microscope cover at 36–38°C. When studying the kinetics of exogenously administered 7-HC, rather than 7-HC resulting from FAOBlue metabolism, 7-HC (2.5 μM, 100 μl/animal) was intravenously injected through the right internal jugular vein. The observations of the 7-HC-injected mice were conducted in the same way as in the FAOBlue-injected mice. No animals reached humane endpoints, and no unexpected adverse events occurred during the experiments.

Multiphoton microscopy

All *in vivo* images were obtained using a Nikon A1R MP+ multiphoton microscope (Nikon, Tokyo, Japan) equipped with a 20× water-immersion objective lens. Excitation was performed using the Chameleon Discovery laser system (Coherent Inc., Santa Clara, CA, USA). A combination of 820 nm excitation and a 450/70 bandpass filter was used to detect

the 7-HC signals. To visualize dextran conjugated with Texas Red™ dye, a combination of 1080 nm excitation and a 593/46 bandpass emission filter was used. Images were obtained continuously before and after the dye injection. For the FAOBlue analyses, the laser power, photomultiplier tube high voltage (PMT HV), and PMT offsets were set to 6.5%, 130 V, and 0 V, respectively. These parameters were set to 7.5 %, 100 V, and 0 V, respectively, for Texas Red™ dye-conjugated dextran. Animals for which data could not be obtained due to body movements during microscopic observation were excluded from the analysis.

Experiments to confirm the fluorescent properties of FAOBlue and 7-HC

To confirm that 7-HC, but not FAOBlue, was fluorescent under our experimental conditions, 7-HC and FAOBlue solutions were dropped on the coverslip and directly observed using a Nikon A1R MP+ multiphoton microscope under the same excitation/emission conditions as *in vivo* imaging for FAO. The samples were diluted using the dilution buffer used in the animal experiments. The fluorescence spectra of FAOBlue and 7-HC were measured in a similar manner by changing the excitation wavelength in 10 nm increments in the range of 710-1020 nm.

Video

The video was prepared using Numpy 1.19.5, a Python library for scientific computing, and Imageio 2.26.0, a Python library that provides an interface for reading and writing a wide range of images. Acquisition of multiphoton microscopy images took 4.2 sec/frame. Videos of FAOBlue- or 7-HC-injected mice were recorded at 10 frames/s, while Texas Red™ dextran-injected mice were recorded at 5 frames/s. Thus, the FAOBlue- or 7-HC-

related video has a rate of 42 ×, whereas the Texas Red™ dextran-related video has a rate of 21 ×.

Real-time PCR

Real-time SYBR Green PCR was performed to quantify mRNA expression using a QuantStudio 7 Flex system (Applied Biosystems, Waltham, MA, USA). The primer sets are shown in Supplemental Table S1. RNA was extracted using TRIzol reagent (Invitrogen) according to the manufacturer's instructions.

Histological analyses

The liver tissues were fixed in 4.0% paraformaldehyde in phosphate-buffered saline. Hematoxylin and eosin (HE) staining of paraffin-embedded sections was carried out using the standard methods. All images of HE-stained sections were obtained using an Eclipse Ni microscope (Nikon, Tokyo, Japan).(15)

Quantification of the multiphoton microscopic images

To quantitatively evaluate the fluorescence intensity, small circular regions of interest (ROIs) with a radius of 4 pixels were placed in the cytoplasmic regions of the images. Since FAO does not occur in the nucleus and FAOBlue metabolite (*i.e.*, 7-HC) is excreted into the bile canaliculi, a 4-pixel ROI was set up to measure fluorescence only in the cytoplasmic region, not overlapping the nuclei and canaliculi regions. At least ten ROIs per animal were measured in the periportal and pericentral regions. ROIs were not selected

with multiple ROIs/cell but one ROI/cell. Because the baseline autofluorescence intensity varied according to the location within the hepatic lobule and by pretreatments, the fluorescence levels were calculated using the mean intensity of the first three frames as 0. Nikon A1R MP+ multiphoton microscopy returned a 12-bit (*i.e.*, 0-4095 grayscale) image, which was converted to an 8-bit (*i.e.*, 0-255 grayscale) image for quantification.(16) The area under the curve (AUC) was calculated by adding the average fluorescence intensity of each region in each frame per animal. The maximum slope was defined as the maximum of the increasing slopes calculated for every five frames of the intensity curve for each animal. The time of the first detection of FAO-derived fluorescence was defined as the point in each ROI when the FAO-derived fluorescence exceeded three standard deviation (SD) values of the first five frames. The time to the fluorescence peak was defined as the average time from the start of observation until reaching the top three points of fluorescence intensity. The rate of decay from the fluorescence peak was calculated by dividing the difference in the fluorescence intensity between at the peak and 7 min by the time between the fluorescent peak and 7 min.

Statistical analyses

A *t*-test was used to evaluate significant differences between two groups. Multiple group comparisons were performed using the Dunnett's test. Statistical significance was defined as $P < 0.05$. All data were analyzed using JMP software (SAS Institute, Cary, NC, USA). All results are presented as means ± SD. The number of replicates is mentioned in the figure legends.

RESULTS

Set up for FAOBlue multiphoton microscopy

To visualize the spatiotemporal dynamics of FAO *in vivo*, we analyzed FAOBlue-injected mice using multiphoton microscopy. Before administering FAOBlue to mice, we tested whether 7-HC could be specifically detected under our microscopic conditions since we have reported that FAOBlue and 7-HC have absorption peaks at 350 and 405 nm in single-photon excitation, respectively.(14) We analyzed the fluorescence spectrum using different two-photon excitation wavelengths (λ_{ex}) and a 415-485 nm emission filter (λ_{em}) (Figure 1A). Under the conditions used in the following animal experiments ($\lambda_{ex}/\lambda_{em}$ = 820/415-485 nm), FAOBlue was not fluorescent, whereas 7-HC increased its fluorescence intensity in a concentration-dependent manner (Figures 1A, B, and Supplemental Figure S1A). We also performed HE-staining of the liver to test whether FAOBlue is toxic. The results showed no obvious difference between the liver of vehicle- and FAOBlue-treated mice (Supplemental Figure S1B).

Identification of hepatic lobular structures under the 820/415-485 nm condition

Constituent cells of the liver form functional segments, namely periportal and pericentral hepatocytes, in the hepatic lobules. Thus, we tested whether FAOBlue can be used to visualize differences in FAO activity for each functional segment rather than the whole organ. Mouse settings for multiphoton microscope analyses are shown in Supplemental Figure S2. Step-by-step instructions and troubleshooting tips are summarized in Supplemental Information. The normal liver showed strong autofluorescence in hepatic stellate cells (bright dots in Figure 1C(a) and (b)).

Hepatocytes were also visualized using autofluorescence, and the autofluorescence level was relatively strong in the areas indicated by the dashed white lines in Figure 1C(a). To make it easier to observe the difference in the autofluorescence levels between the area enclosed by the dashed line and the rest, a figure in which the grayscale has been adjusted is shown in Figure 1C(c). It has been reported that autofluorescence of hepatocytes helps identify the anatomy of the lobule. To determine this anatomy under the $\lambda_{ex}/\lambda_{em}$ = 820/415-485 nm condition, we analyzed which part of the hepatic lobule the area enclosed by the white dashed line corresponds to. Analysis of Texas Red™ dextran (70 kDa)-injected mice revealed that blood flowed toward the area surrounded by the white dashed line (Figure 1C(d)-(g), and Supplemental Video S1). Therefore, the enclosed areas are the pericentral regions of the hepatic lobules.

Spatiotemporal quantification of FAO activity in the liver revealed a difference in FAO activation mode between pemafibrate and fasting

To visualize FAO activity in the liver, six- to seven-week-old male C57BL/6J mice were randomly divided into five groups: Ctrl, Pema, Fasting_24h, Fasting_72h, and Eto (Figure 2). Mice in the Ctrl group received no pretreatment. Mice in the Pema and Eto groups were pretreated with pemafibrate, a selective peroxisome proliferator-activated receptor α (PPARα) modulator, and etomoxir, an inhibitor of mitochondrial carnitine palmitoyl transferase 1 (CPT1), respectively. Mice in the Fasting_24h and Fasting_72h groups were fasted for 24 or 72 hours, respectively. Since PPARα is a key regulator of gene expression involved in FAO, and fasting triggers fat mobilization from adipose tissues, we anticipated FAO activation in both the Pema and the two fasting groups.(17, 18) Conversely, as CPT1 is the rate-limiting enzyme for FAO, we expected FAO to be suppressed in the Eto

group.(19) The FAO activity was visualized with a single intravenous injection of FAOBlue. Representative liver images of the Ctrl and pretreated mice are shown in Figure 2 and Supplemental Video S2.

We quantified fluorescent intensities of hepatocytes by setting circular ROIs with a radius of 4 pixels (Figure 3 and Supplemental Figure S3A). It was previously reported that FAOBlue-treated HepG2 cells gradually increased FAO-derived fluorescence in a time-dependent manner up to 30 min, however, the fluorescent signal of the periportal region in the Ctrl, Pema, Fasting_24h, and Fasting_72h groups peaked much earlier (Figures 2, 3A and Supplemental Video S2).(14) Because CPT1 activity in HepG2 cells has been shown to be lower than that in parenchymal hepatocytes, low CPT1 activity in HepG2 cells may explain the reason why FAO-derived fluorescence in HepG2 cells increased slower than *in vivo*.(20) Strong fluorescence signals were detected in the bile canaliculi at about the same time that FAO activity was observed in the hepatocytes, suggesting that the 7-HC was actively excreted into the canaliculi (Supplemental Figure S3B). No increase in fluorescence was observed in the Eto group, confirming that FAOBlue specifically detected mitochondrial FAO *in vivo*. The AUCs in Figure 3A for the Pema, Fasting_24h, and Fasting_72h groups were higher than those of the Ctrl group in both the periportal and pericentral regions, though the elevation in the pericentral region of the Fasting_24h group was marginal (Figure 3B). The periportal AUCs were higher than the pericentral AUCs in all groups, except for the Eto group (Figure 3A and Supplemental Figure S3C). We also measured the increasing slope of the intensity curve every five frames and determined the maximum intensity slope for each animal. The Pema and Fasting_72h groups, but not Fasting_24h group, showed increased maximum slopes of the intensity curve compared with the Ctrl group in both hepatic lobular regions (Figure 3C). The maximum intensity slope of the periportal region was higher than that of the pericentral region in all groups

except for the Eto group (Supplemental Figure S3D). The differences in AUC and maximum slope between the Ctrl and Eto groups were significant in the periportal region but not in the pericentral region, showing that FAO in the Ctrl group occurred mainly in the periportal region, with few FAO in the pericentral region (Figures 3B and 3C). Although the pemafibrate and fasting treatments both stimulate FAO, FAOBlue-based spatiotemporal analyses revealed that these interventions activate FAO differently. The first detection of FAO-derived fluorescence in the Pema group was significantly earlier than that in the Ctrl, but not different between the Fasting_24h or Fasting_72h group and the Ctrl groups (Figures 3A and 3D). Real-time PCR analyses of FAO-related genes in the liver showed that the levels of *Cpt1a* were elevated in the Pema, Fasting_24h and Fasting_72h groups compared to that in the Ctrl group (Figure 3E). *Cpt1* mRNA expression was also elevated in the Eto group, which seems be a compensatory response to FAO suppression. The mRNA level of *Ppara*, encoding PPARα, the key regulator of FAO, was elevated in the FAO-stimulated groups, *i.e.*, the Pema, Fasting_24h, and Fasting_72h groups, but the downstream gene expression levels were not uniform among the groups. *Cpt2* mRNA expression was elevated in the Pema and Fasting_24h groups but not in the Fasting_72h group. The expression levels of *Ppargc1a*, encoding peroxisome proliferator-activated receptor gamma coactivator 1-alpha (PGC1a), a master regulator of mitochondrial biogenesis, were elevated in the Fasting_24h group but not in the Pema and Fasting_72h groups. The levels of *Cd36*, a molecule that facilitates fatty acid uptake, were induced by pemafibrate, but not by fasting. Therefore, the earlier FAO detection time in the Pema group may be due to enhanced fatty acid uptake by hepatocytes.

The results shown in Figures 1-3 indicated that FAOBlue is useful for visualizing FAO activation by various stimulations, as well as for illustrating the differences in FAO activities between the periportal and pericentral regions of the liver. However, to make an

accurate assessment, there were several additional aspects that needed to be clarified. For example, if the speed at which 7-HC is excreted to the bile canaliculi varies among the experimental groups, group comparisons might not be conducted appropriately. Furthermore, 7-HC, resulting from FAO in other organs and circulating in the blood vessels, might be taken up primarily in the periportal region, leading to the results shown in Figures 2 and 3. To address these issues, we analyzed the kinetics of 7-HC by administrating 7-HC through the right jugular vein. In this experiment, the 7-HC dosage was set at 0.25 nmol/animal (2.5 μM solution, 100 μl/animal), a reduction from the FAOBlue amount of 6.25 nmol/animal (62.5 μM solution, 100 μl/animal) used in the experiments shown in Figures 2 and 3. The purpose of this reduction was to determine whether the amount of 7-HC administered into the vasculature, even at a dosage that would result in fluorescent intensity comparable to that in the periportal region of the Ctrl group treated with FAOBlue, would be sufficient to reach the pericentral region. As a result, the fluorescence intensity increased in both the periportal and pericentral regions immediately after the 7-HC administration (Figures 4, 5, and Supplemental Video S3). The AUC of the fluorescence curve, the time to peak fluorescence, and the rate of decay from the fluorescence peak were similar, irrespective of pretreatment or whether in the periportal or pericentral region (Figures 4, 5, Supplemental Figure S4, and Supplemental Video 3). Therefore, the comparisons of FAO among groups and between pericentral and periportal regions can be conducted appropriately using FAOBlue.

DISCUSSION

This study demonstrated that FAOBlue is a useful tool for the spatiotemporal quantification of FAO in mice liver. Our method shows that (1) FAO occurs mainly in the

periportal region; (2) the two FAO-activating stimuli, pemafibrate and fasting for 72 hours, activate FAO in both the periportal and pericentral regions in terms of FAO quantity and velocity, which are expressed by the AUCs and maximum increasing slope of the FAOBlue-derived fluorescence intensity curve, respectively; (3) The Fasting_24h and Fastign_72h groups increas the FAO quantity compared to the Ctrl group, with the pericentral region of the Fasting_24h group showing marginal significance. The FAO velocity increases in the Fasting_72h group, but not in the Fasting_24h group, indicating that the pattern of FAO varies with the duration of fasting; and (4) both pemafibrate and fasting are FAO-activating stimuli, but the time of first detection of FAO-derived fluorescence is different. Our method is widely applicable because it is simple and uses a multiphoton microscope to observe the FAOBlue-injected mice.

Spatial heterogeneity of hepatocytes has been reported since the early 20th century. Kater *et al*. showed gradients along the porto-central axis in deposition levels of glycogen and fat, as well as mitochondrial morphology in 1933.(21) Deane demonstrated that periportal hepatocytes have larger mitochondria and less deposition of fat and coined the term ‘zonation’ in 1944.(22) Following these pioneering morphology-based studies, Braeuning *et al*. analyzed the overall picture of mRNA expression levels in the hepatic zone using microarray. They isolated periportal and pericentral hepatocytes using the digitonin-collagenase perfusion technique and showed that periportal hepatocytes express higher levels of FAO-related genes than pericentral hepatocytes.(23) More recently, Halpern *et al.* performed single-cell RNA sequencing of the mouse liver and revealed the zonation profiles of liver gene expressions with high spatial resolution.(24) Although these studies have led to considerable advances in liver research, the mere expression of FAO-related enzymes does not necessarily translate into FAO activation. The hepatic zonation was dynamic rather than static. For example, Guzmán *et al*. showed that oxidation of ^{14}C-

labeled palmitate was very flexible and changed markedly with the animal's physiological status.(25) Therefore, evaluating the FAO activity directly is essential. Our method is superior to previous methods in terms of radioisotope-free and high spatiotemporal resolution.

FAOBlue has a structure consisting of a fatty acid with a carbon chain length of nine (C9) and 7-HC. In contrast to long-chain fatty acids, whose conversion to long-chain acyl-carnitine species via CPT1 is required for mitochondrial transport, short- and medium-chain fatty acids can enter mitochondria in a carnitine-independent manner. However, CPT1 was required for the β-oxidation of FAOBlue, whose carbon chain length belongs to the medium chain. This is not simply because C9 bound to 7-HC resulted in a longer structure; we have previously shown that C5 (short-chain) bound 7-HC probe scarcely underwent β-oxidation even in the absence of etomoxir.(14) We have also demonstrated that C9 probe that possesses rhodol or naphthalimide as a fluorophore did not undergo any structural change upon incubation with the HepG2 cells.(14) Therefore, the combination of C9 and 7-HC was optimal for CPT-1-dependent mitochondrial transport, though the structural basis remains uncertain. Acyl-CoA dehydrogenases (ACADs) are enzymes that catalyze the initial double-bound introduction step of mitochondrial FAO. Based on substrate preference, ACADs are classified into several types: short-, medium-, long-, and very long-chain ACADs. They are most active with 4C-, 8C-, 14C-, and 16C-substrates, respectively.(26) Because substrates whose acyl chain length is too long for a particular ACAD are excluded, while short-chain substrates bind weakly to ACADs specific for longer substrates, the initial introduction of double-bound to FAOBlue is likely mediated by medium- or longer-chain ACADs.(26) In the later cycles of FAO, short-chain ACAD might also be responsible for the double-bound introduction.

The results shown in Figures 4, 5, and Supplemental Figure S4 showed that there are no differences in the excretion of 7-HC from hepatocytes to the bile canaliculi, either

among the experimental groups or between the periportal and pericentral regions. This finding corroborates the validity of the group and the region comparisons depicted in Figure 3B-D and Supplemental Figure S3C-D. However, the fluorescence observed in Figure 3A, following the peak period of fluorescence intensity, is likely to represent the fluorescence of 7-HC produced by FAO at earlier phases and not yet excreted, rather than the fluorescence of 7-HC generated by FAO of FAOBlue at that particular time point.

This study has several limitations. First, FAOBlue is unsuitable for observing deep in organs because the fluorescence wavelength of 7-HC is short. Second, although our data suggested that 7-HC generated in the liver was excreted mainly through the canaliculi, details of how 7-HC generated in other organs is distributed or excreted are still unclear. These issues should be addressed in future studies.

In conclusion, we demonstrated that observing FAOBlue-injected mice by multiphoton microscopy is helpful for analyzing the spatiotemporal dynamics of FAO. It also helps explore new insights into FAO.

DATA AVAILABILITY

Lead Contact

- Further information and requests for resources and reagents should be directed to and will be fulfilled by the Lead Contact, Isao Matsui (matsui@kid.med.osaka-u.ac.jp).

Materials availability

- This study did not generate any unique materials.

Data and Code Availability

- The image quantification code is available at https://github.com/NephrologyOsakaUniv/2023_FAOBlue/blob/main/2023_FAO_quantification.ipynb

SUPPLEMENTAL MATERIAL

Supplemental Information and legends, Supplemental Videos S1, S2 and S3: https://figshare.com/s/df059d995711463d359a

ACKNOWLEDGMENTS

The authors would sincerely like to thank Naoko Horimoto for her technical assistance on this manuscript, as well the Center of Medical Research and Education, Osaka University Graduate School of Medicine. We are also grateful the Nikon Imaging Center at Osaka University for their assistance with multiphoton microscopy, image acquisition, and analysis.

GRANTS

This work was supported by The Kidney Foundation, Japan Grant JKFB21-9 (To Yusuke Katsuma).

DISCLOSURES

The authors declare no competing interest.

AUTHOR CONTRIBUTIONS

AM, IM, SU, YK conceived and designed research; AM, YK, SY, HO, AI, TY performed experiments, analyzed data, interpreted results of experiments; AM, IM prepared figures, AM, IM drafted manuscript; IM, SU, AO, KI edited and revised manuscript; IM, AO, YI approved final version of manuscript.

REFERENCES

1. **Houten SM**, **Violante S**, **Ventura F V.**, **Wanders RJA**. The Biochemistry and Physiology of Mitochondrial Fatty Acid β-Oxidation and Its Genetic Disorders. *Annu Rev Physiol* 78: 23–44, 2016. doi: 10.1146/ANNUREV-PHYSIOL-021115-105045.

2. **Li Z**, **Zhang H**. Reprogramming of glucose, fatty acid and amino acid metabolism for cancer progression. *Cellular and Molecular Life Sciences 2015 73:2* 73: 377–392, 2015. doi: 10.1007/S00018-015-2070-4.

3. **Zhang L**, **Keung W**, **Samokhvalov V**, **Wang W**, **Lopaschuk GD**. Role of fatty acid uptake and fatty acid beta-oxidation in mediating insulin resistance in heart and skeletal muscle. *Biochim Biophys Acta* 1801: 1–22, 2010. doi: 10.1016/J.BBALIP.2009.09.014.

4. **Kang HM**, **Ahn SH**, **Choi P**, **Ko YA**, **Han SH**, **Chinga F**, **Park ASD**, **Tao J**, **Sharma K**, **Pullman J**, **Bottinger EP**, **Goldberg IJ**, **Susztak K**. Defective fatty acid oxidation in renal tubular epithelial cells has a key role in kidney fibrosis development. *Nature Medicine 2014 21:1* 21: 37–46, 2014. doi: 10.1038/nm.3762.

5. **Yamamoto T**, **Takabatake Y**, **Minami S**, **Sakai S**, **Fujimura R**, **Takahashi A**, **Namba-Hamano T**, **Matsuda J**, **Kimura T**, **Matsui I**, **Kaimori JY**, **Takeda H**, **Takahashi M**, **Izumi Y**, **Bamba T**, **Matsusaka T**, **Niimura F**, **Yanagita M**, **Isaka Y**. Eicosapentaenoic acid attenuates renal lipotoxicity by restoring autophagic flux. *Autophagy* 17: 1700–1713, 2021. doi: 10.1080/15548627.2020.1782034.

6. **Mori D**, **Matsui I**, **Shimomura A**, **Hashimoto N**, **Matsumoto A**, **Shimada K**, **Yamaguchi S**, **Oka T**, **Kubota K**, **Yonemoto S**, **Sakaguchi Y**, **Takahashi A**, **Shintani Y**, **Takashima S**, **Takabatake Y**, **Hamano T**, **Isaka Y**. Protein carbamylation exacerbates vascular calcification. *Kidney Int* 94, 2018. doi: 10.1016/j.kint.2018.01.033.

7. **Chace DH**, **Kalas TA**, **Naylor EW**. Use of tandem mass spectrometry for multianalyte screening of dried blood specimens from newborns. *Clin Chem* 49: 1797–1817, 2003. doi: 10.1373/CLINCHEM.2003.022178.

8. **Nomura M**, **Liu J**, **Rovira II**, **Gonzalez-Hurtado E**, **Lee J**, **Wolfgang MJ**, **Finkel T**. Fatty acid oxidation in macrophage polarization. *Nature Immunology 2016 17:3* 17: 216–217, 2016. doi: 10.1038/ni.3366.

9. **Manning NJ**, **Olpin SE**, **Pollitt RJ**, **Webley J**. A comparison of [9,10-3H]palmitic and [9,10-3H]myristic acids for the detection of defects of fatty acid oxidation in intact cultured fibroblasts. *J Inherit Metab Dis* 13: 58–68, 1990. doi: 10.1007/BF01799333.

10. **Guzman M**, **Bijleveld C**, **Geelen MJH**. Flexibility of zonation of fatty acid oxidation in rat liver. *Biochem J* 311: 853–860, 1995. doi: 10.1042/BJ3110853.

11. **Ito M**, **Adachi-Akahane S**. Inter-organ communication in the regulation of lipid metabolism: focusing on the network between the liver, intestine, and heart. *J Pharmacol Sci* 123: 312–317, 2013. doi: 10.1254/JPHS.13R09CP.

12. **Whitehead A**, **Krause FN**, **Moran A**, **MacCannell ADV**, **Scragg JL**, **McNally BD**, **Boateng E**, **Murfitt SA**, **Virtue S**, **Wright J**, **Garnham J**, **Davies GR**, **Dodgson J**, **Schneider JE**, **Murray AJ**, **Church C**, **Vidal-Puig A**, **Witte KK**, **Griffin JL**, **Roberts LD**. Brown and beige adipose tissue regulate systemic metabolism through a metabolite interorgan signaling axis. *Nature Communications 2021 12:1* 12: 1–21, 2021. doi: 10.1038/s41467-021-22272-3.

13. **Cunningham RP**, **Porat-Shliom N**. Liver Zonation - Revisiting Old Questions With New Technologies. *Front Physiol* 12, 2021. doi: 10.3389/FPHYS.2021.732929.

14. **Uchinomiya S**, **Matsunaga N**, **Kamoda K**, **Kawagoe R**, **Tsuruta A**, **Ohdo S**, **Ojida A**. Fluorescence detection of metabolic activity of the fatty acid beta oxidation pathway in living cells. *Chem Commun (Camb)* 56: 3023–3026, 2020. doi: 10.1039/C9CC09993J.

15. **Matsui I**, **Hamano T**, **Mikami S**, **Inoue K**, **Shimomura A**, **Nagasawa Y**, **Michigami T**, **Ohnishi T**, **Fujii N**, **Nakano C**, **Kusunoki Y**, **Kitamura H**, **Iwatani H**, **Takabatake Y**, **Kaimori J**, **Matsuba G**, **Okoshi K**, **Kimura-Suda H**, **Tsubakihara Y**, **Rakugi H**, **Isaka Y**. Retention of fetuin-A in renal tubular lumen protects the kidney from nephrocalcinosis in rats. *American Journal of Physiology-Renal Physiology* 304: F751–F760, 2013. doi: 10.1152/ajprenal.00329.2012.

16. **Matsumoto A**, **Matsui I**, **Katsuma Y**, **Yasuda S**, **Shimada K**, **Namba-Hamano T**, **Sakaguchi Y**, **Kaimori J**, **Takabatake Y**, **Inoue K**, **Isaka Y**. Quantitative Analyses of Foot Processes, Mitochondria, and Basement Membranes by Structured Illumination. *Kidney Int Rep* 6: 1923–1938, 2021. doi: 10.1016/j.ekir.2021.04.021.

17. **Pawlak M**, **Lefebvre P**, **Staels B**. Molecular mechanism of PPARα action and its impact on lipid metabolism, inflammation and fibrosis in non-alcoholic fatty liver disease. *J Hepatol* 62: 720–33, 2015. doi: 10.1016/j.jhep.2014.10.039.

18. **Rakhshandehroo M**, **Knoch B**, **Müller M**, **Kersten S**. Peroxisome proliferator-activated receptor alpha target genes. *PPAR Res* 2010, 2010. doi: 10.1155/2010/612089.

19. **Schlaepfer IR**, **Joshi M**. CPT1A-mediated Fat Oxidation, Mechanisms, and Therapeutic Potential. *Endocrinology* 161, 2020. doi: 10.1210/endocr/bqz046.

20. **Agius L**. Metabolic interactions of parenchymal hepatocytes and dividing epithelial cells in co-culture. *Biochem J* 252, 1988. doi: 10.1042/bj2520023.

21. **Kater JM**. Comparative and experimental studies on the cytology of the liver. *Für Zellforsch Mikrosk Anat* 17: 217–246, 1933.

22. **Deane HW**. A cytological study of the diurnal cycle of the liver of the mouse in relation to storage and secretion. *Anat Rec* 88: 39–65, 1944.

23. **Braeuning A**, **Ittrich C**, **Köhle C**, **Hailfinger S**, **Bonin M**, **Buchmann A**, **Schwarz M**. Differential gene expression in periportal and perivenous mouse hepatocytes. *FEBS Journal* 273: 5051–5061, 2006. doi: 10.1111/J.1742-4658.2006.05503.X.

24. **Halpern KB**, **Shenhav R**, **Matcovitch-Natan O**, **Tóth B**, **Lemze D**, **Golan M**, **Massasa EE**, **Baydatch S**, **Landen S**, **Moor AE**, **Brandis A**, **Giladi A**, **Stokar-Avihail A**, **David E**, **Amit I**, **Itzkovitz S**. Single-cell spatial reconstruction reveals global division of labor in the mammalian liver. *Nature* 542: 352, 2017. doi: 10.1038/NATURE21065.

25. **Guzman M**, **Bijleveld C**, **Geelen MJH**. Flexibility of zonation of fatty acid oxidation in rat liver. *Biochem J* 311: 853–860, 1995. doi: 10.1042/BJ3110853.

26. **Mander L**, **Liu HW**. Comprehensive Natural Products II: Chemistry and Biology. 2010.

FIGURE LEGENDS

Figure 1. Multiphoton microscope set up

(A) Fluorescence spectra of FAOBlue and 7-Hydroxycoumarin-3-(N-(2-hydroxyethyl))-carboxamide (7-HC) under the excitation of a two-photon laser. The fluorescence intensity of FAOBlue (62.5 μM) or 7-HC (0.3125 μM) dissolved in a dilute buffer was measured using a two-photon microscope (λ_{em} = 415-585 nm). The horizontal axis represents the excitation wavelength of the two-photon microscope. The original microscopic images were 12-bit

grayscale but were converted to 8-bit grayscale (0–255 scale) for analysis. The vertical axis of the graph represents the average grayscale of the acquired images (*i.e.*, fluorescence intensity) (N = 5 in each measurement). (B) The signal intensities of the dilution buffer, FAOBlue, and 7-HC solution ($\lambda_{ex}/\lambda_{em}$ = 820/415-485 nm). The regression line for 7-HC was drawn using measurements within the concentration range of 0 to 0.625 μM (N = 5 in each measurement: R^2 = 0.9916). All results are presented as the means ± standard deviations (SDs). (C) (a)–(d) Representative liver images at baseline and (e)-(g) the first frame in which injected Texas Red™ dextran (70 kDa) appeared (Scale bars: 100 μm). See Supplemental Video S1. (a) and (c)-(g) are observations of the same region. The orange square in (a) was enlarged in (b). (a) White dashed circles indicate areas where hepatocytes have relatively strong autofluorescence. To make it easier to see the difference in hepatocyte autofluorescence in (a), the signal range of 0-50 in (a) was visualized in (c). In addition to the area whose signal intensity was 50 in (a), the area whose signal intensity was between 51 and 255 in (a) was also represented in white in (c). (f) Brightness-enhanced image of (e). The brightness-enhanced image was prepared in a similar manner to (c). (g) The images in (c) and (f) were superimposed with green and red pseudo-colors, respectively.

Figure 2. Spatiotemporal visualization of FAO activity in the liver

FAO activities of the liver in the (A–C) Ctrl, (D–F) Pema, (G–I) Fasting_24h, (J–L) Fasting_72h, and (M-O) Eto groups were visualized at 0, 2, and 7 min ($\lambda_{ex}/\lambda_{em}$ = 820/415-485 nm). See Supplemental Video S2. Multiphoton microscopy observation began at 0 min. FAOBlue was injected at 0.5 min. Representative microscopic images are shown. White dashed circles in (A), (D), (G), (J) and (M) indicate pericentral regions (Scale bars: 100 μm). FAO: fatty acid β-oxidation, Ctrl: Control, Pema: Pemafibrate, Fasting_24h: fasting for 24 hours, Fasting_72h: fasting for 72 hours, Eto: Etomoxir.

Figure 3. Spatiotemporal quantification of FAO activity in the liver and real-time PCR analyses of FAO-related genes

(A–D) FAO activities of the liver in the Ctrl, Pema, Fasting_24h, Fasting_72h, and Eto groups shown in Figure 2 and Supplemental Video S2 were spatiotemporally quantified. (A) Time courses of the fluorescence intensity of hepatocytes in the periportal and pericentral regions. Black arrows indicate the time point when FAOBlue was injected. (B) AUCs of (A) are shown. (C) Maximum increasing slope of (A) in each animal. (D) Time of first detection of FAO-derived fluorescence in each animal. (E) Real-time PCR analyses of FAO-related genes in the liver. All results are presented as a scatter plot with means ± SDs (N = 5-8 biological replicates in each group: * $P < 0.05$, ** $P < 0.01$, Dunnett's test). n/a: not available, ns: not significant, Ref: reference, AUC: area under the curve.

Figure 4. Spatiotemporal visualization of liver fluorescence after injection of 7-HC through the right jugular vein

Mice were pretreated as in the FAOBlue administration experiments and then injected with 7-HC through the right jugular vein. (A–C) Ctrl, (D–F) Pema, (G–I) Fasting_24h, (J–L) Fasting_72h, and (M-O) Eto groups. Representative microscopic images at 0,1, and 7 minutes are shown, with 7-HC being injected at 0.5 minutes ($\lambda_{ex}/\lambda_{em}$ = 820/415-485 nm). White dashed circles indicate pericentral regions (Scale bars: 100 μm). See Supplemental Video S3.

Figure 5. Spatiotemporal quantification of liver fluorescence after injection of 7-HC through the right jugular vein

(A–D) Fluorescent intensity of the liver in the Ctrl, Pema, Fasting_24h, Fasting_72h, and Eto groups shown in Figure 4 and Supplemental Video S3 were spatiotemporally quantified. (A) Time courses of the fluorescence intensity of hepatocytes in the periportal and pericentral regions. Black arrows indicate the time point when 7-HC was injected. (B) AUCs of (A) are shown. (C) The time to peak fluorescence and (D) the rate of decay from the fluorescence peak are presented (N = 3 biological replicates in each group: ns, not significant: Dunnett's test).

Figure 1

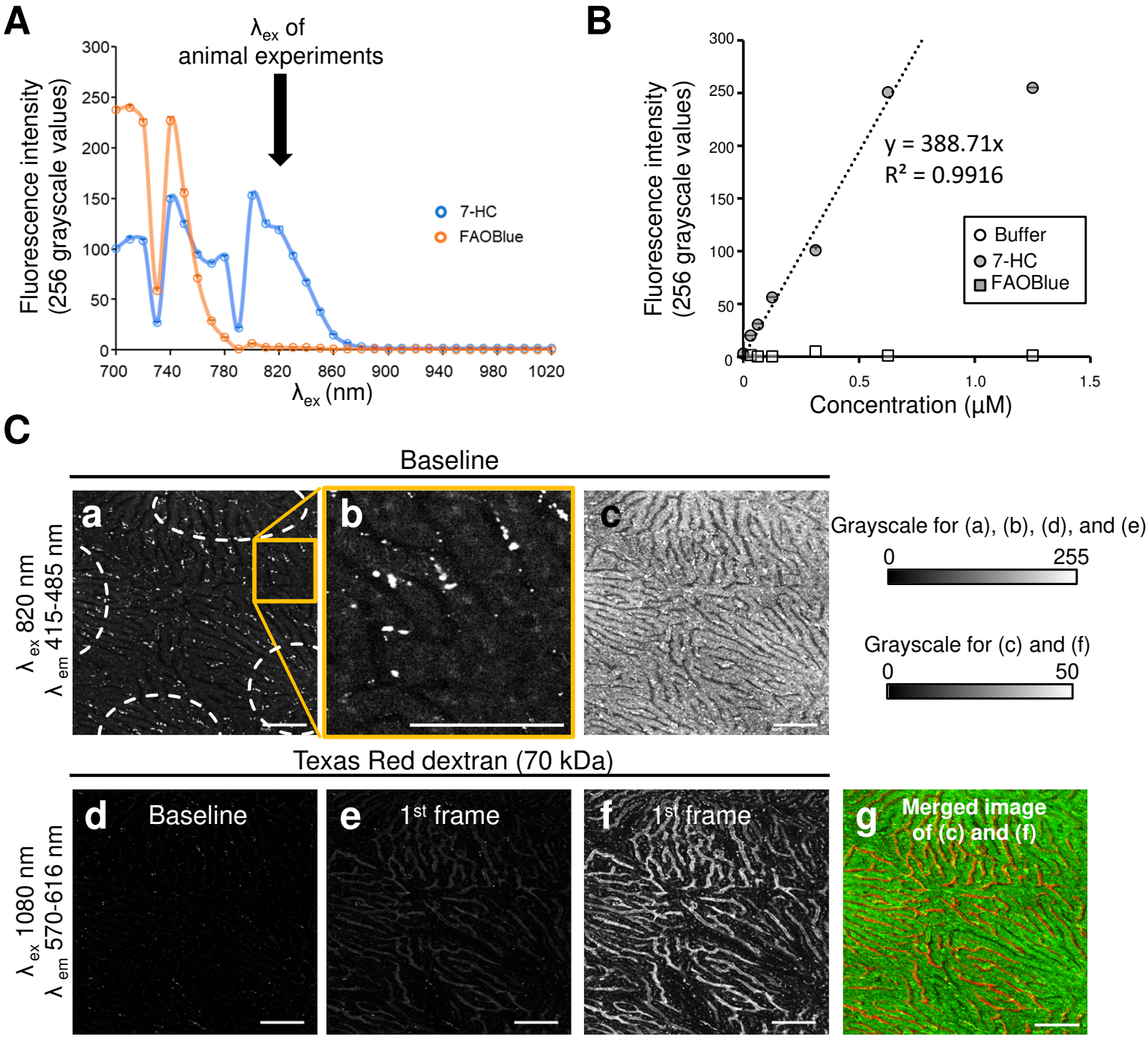
A
λex of
animal experiments
Fluorescence intensity
(256 grayscale values)
λex (nm)
7-HC
FAOBlue
B
Fluorescence intensity
(256 grayscale values)
y = 388.71x
R² = 0.9916
Buffer
7-HC
FAOBlue
Concentration (μM)
C
Baseline
λex 820 nm
λem 415-485 nm
a
b
c
Grayscale for (a), (b), (d), and (e)
0
255
Grayscale for (c) and (f)
0
50
Texas Red dextran (70 kDa)
λex 1080 nm
λem 570-616 nm
d
Baseline
e
1st frame
f
1st frame
g
Merged image
of (c) and (f)

Figure 2

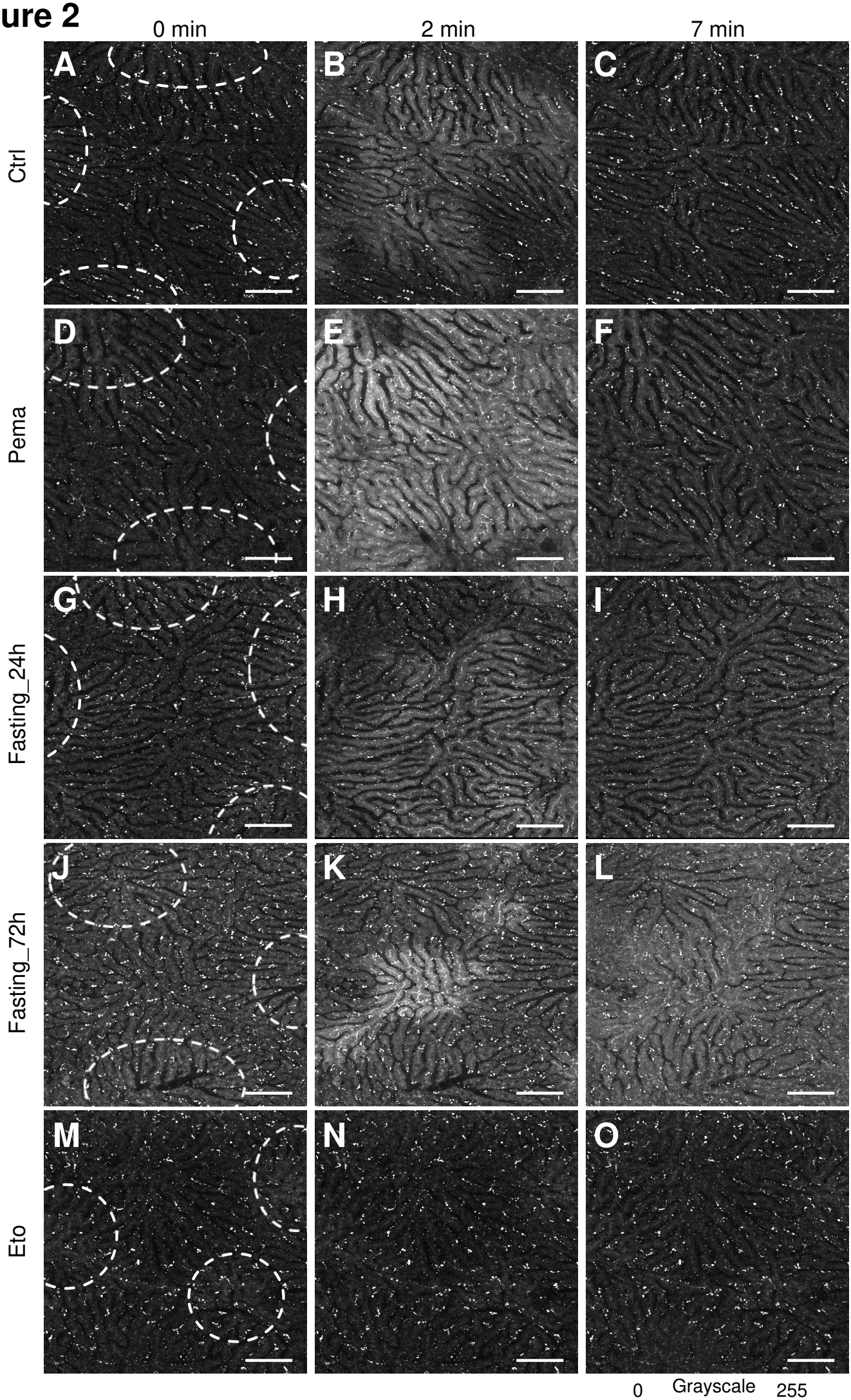
0 min
2 min
7 min
Ctrl
Pema
Fasting_24h
Fasting_72h
Eto
A
B
C
D
E
F
G
H
I
J
K
L
M
N
O
0
Grayscale
255

Figure 3

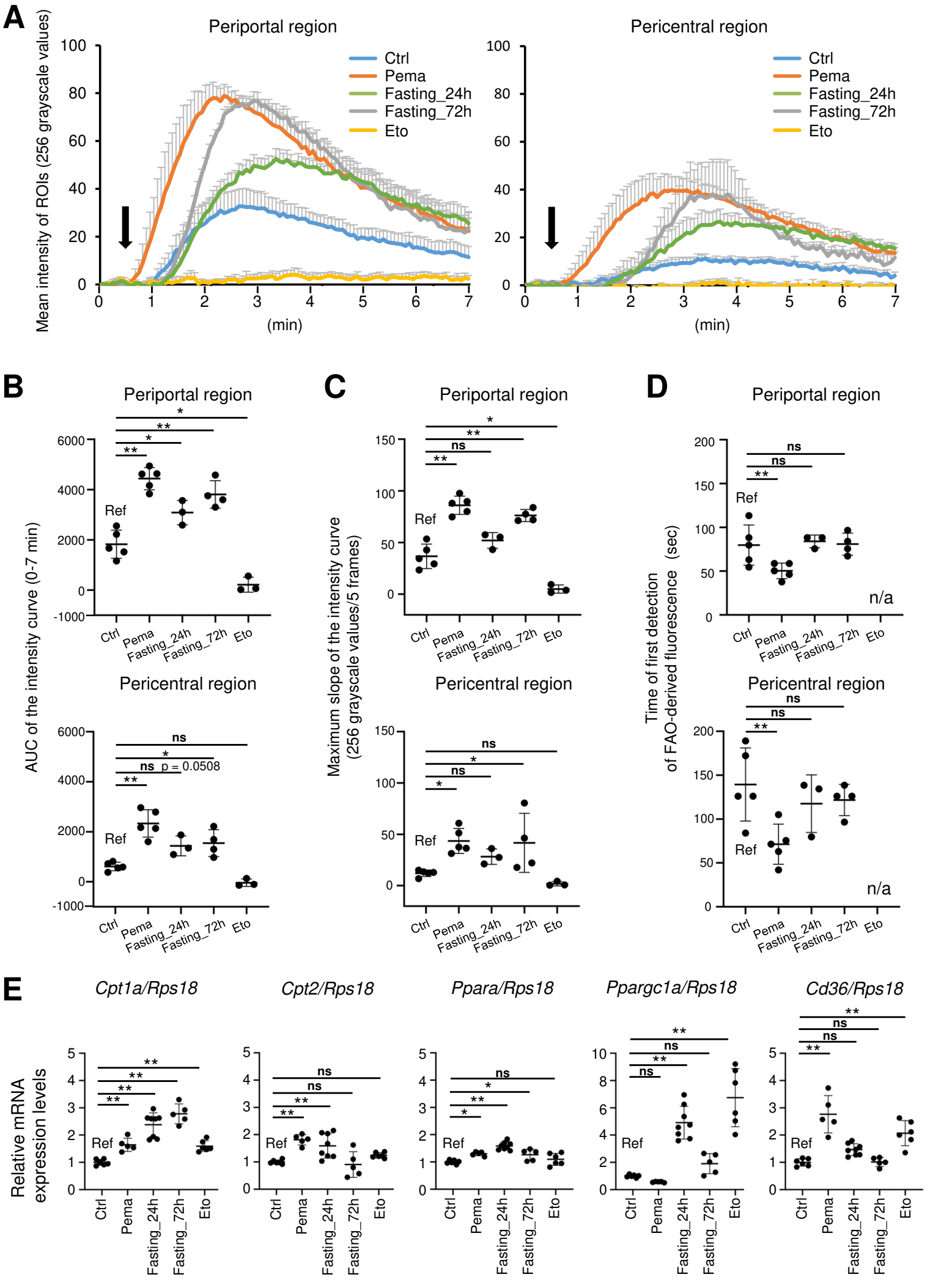
A
Periportal region
Pericentral region
Ctrl
Pema
Fasting_24h
Fasting_72h
Eto
Mean intensity of ROIs (256 grayscale values)
(min)
B
AUC of the intensity curve (0-7 min)
C
Maximum slope of the intensity curve (256 grayscale values/5 frames)
D
Time of first detection of FAO-derived fluorescence (sec)
n/a
ns
p = 0.0508
Ref
E
Cpt1a/Rps18
Cpt2/Rps18
Ppara/Rps18
Ppargc1a/Rps18
Cd36/Rps18
Relative mRNA expression levels

Figure 4

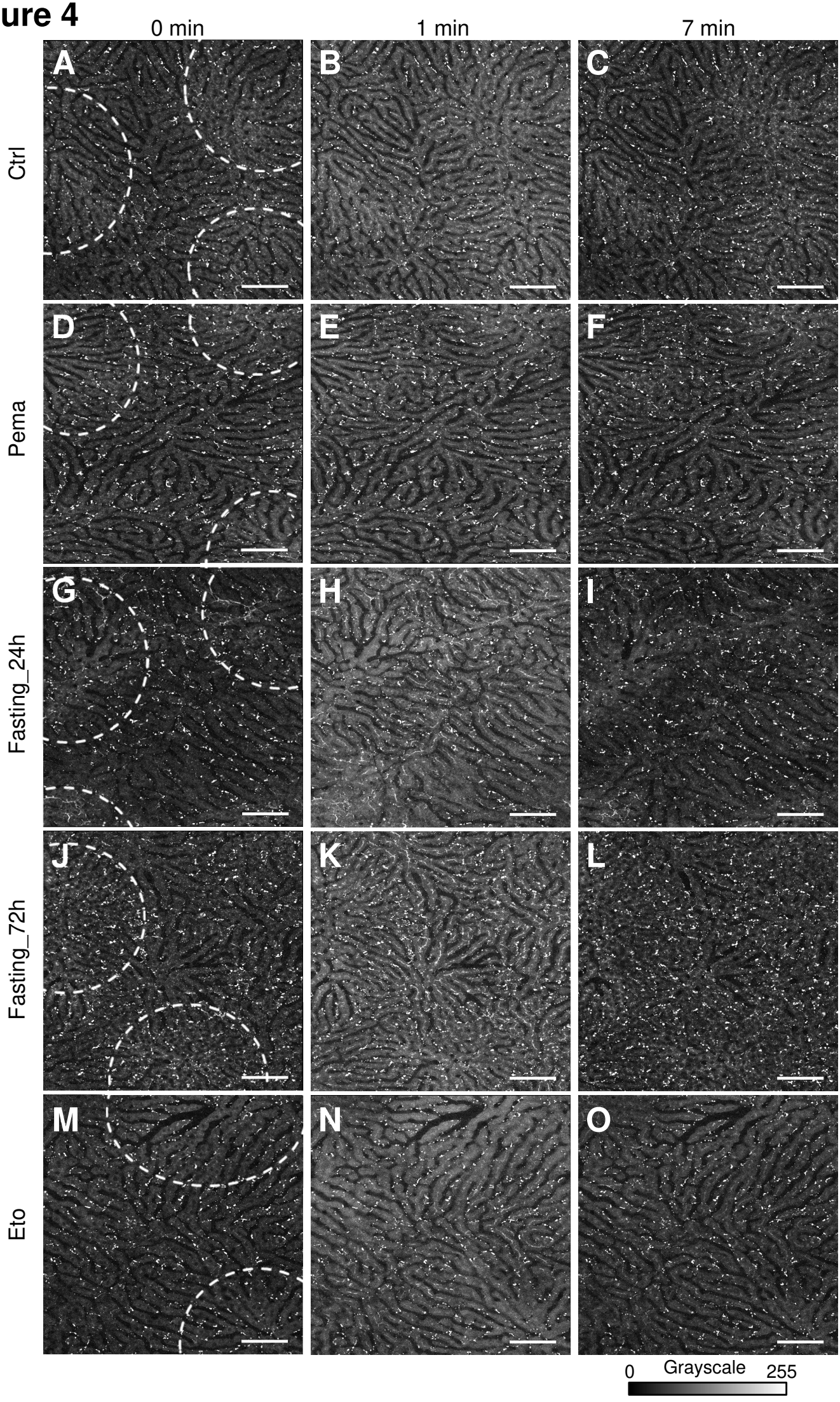
0 min
1 min
7 min
Ctrl
Pema
Fasting_24h
Fasting_72h
Eto
A
B
C
D
E
F
G
H
I
J
K
L
M
N
O
0
Grayscale
255

Figure 5

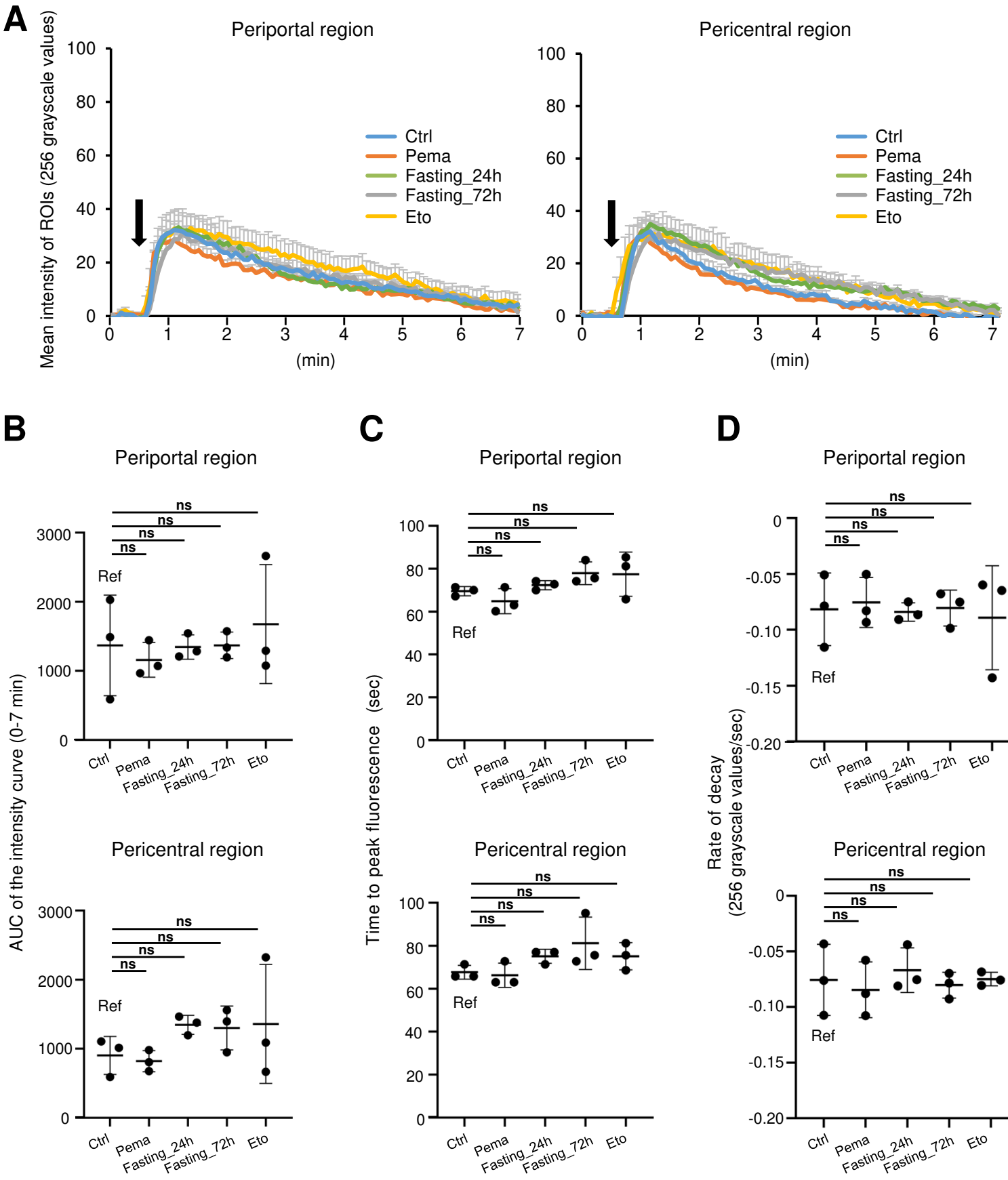
A
Periportal region
Pericentral region
Mean intensity of ROIs (256 grayscale values)
(min)
Ctrl
Pema
Fasting_24h
Fasting_72h
Eto
B
C
D
AUC of the intensity curve (0-7 min)
Time to peak fluorescence (sec)
Rate of decay (256 grayscale values/sec)
Ref
ns

Spatiotemporally quantitative *in vivo* imaging of mitochondrial fatty acid β-oxidation at cellular-level resolution in mice

METHODS

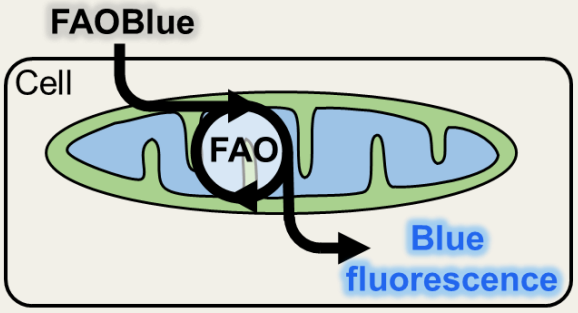

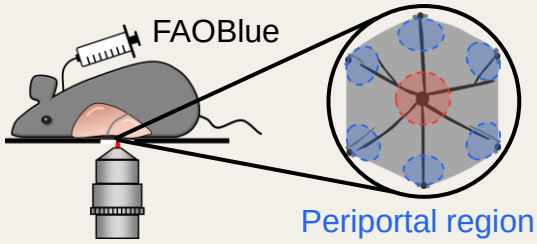

Multiphoton microscopy

OUTCOME *In vivo* quantification of FAO activity

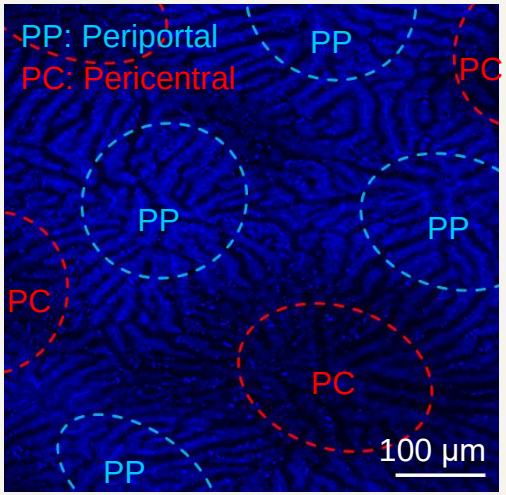

Spatial resolution
cellular-level

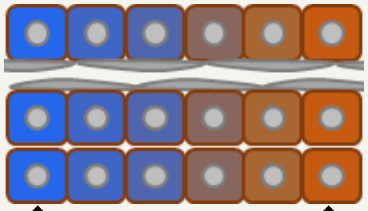

PP hepatocytes PC hepatocytes

Temporal resolution
Seconds-level

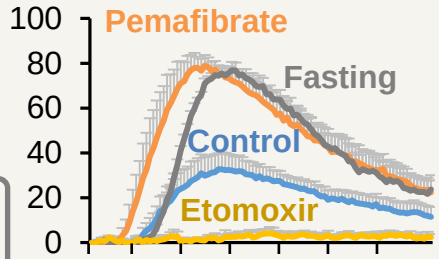

You can evaluate

- FAO activity
- FAO velocity
- FAO induction time

in each cell in live animals.

CONCLUSION

FAOBlue-based multiphoton imaging
is useful for evaluating spatiotemporal FAO dynamics.